

THS



This is to certify that the

thesis entitled

A Bond-Graph Approach to Finite Element Methods

presented by

Craig Wendel Galer

has been accepted towards fulfillment of the requirements for

M.S. degree in Mech. Eng.

R. C. Roenbey

Major professor

Date ____11/10/78

O-7639

A BOND-GRAPH APPROACH TO FINITE ELEMENT METHODS

Ву

Craig Wendel Galer

A THESIS

Submitted to

Michigan State University
in partial fulfillment of the requirements

for the degree of

MASTER OF SCIENCE

Department of Mechanical Engineering

ABSTRACT

52

A BOND-GRAPH APPROACH TO FINITE ELEMENT METHODS

bу

Craig Wendel Galer

Bond-graph techniques are applied in finite-element analysis. A procedure is developed for constructing a bond-graph model for constant-strain triangular elements from their stiffness matrices. Causality is proposed as a useful tool in deriving the response of finite-element assemblies.

A comparison of bond-graph and standard finite-element methods is also made, and some simple extensions of the bond-graph method are proposed.

ACKNOWLEDGEMENTS

Many thanks to Professor Ronald C. Rosenberg for all his assistance and guidance both on this thesis and throughout my M.S. program.

Thanks also to all the friendly people in Mechanical Engineering, who helped make my graduate studies a most enjoyable experience.

Humble thanks to my parents, who "Trained me up in the way I should go" (Proverbs 22:6).

And deepest gratitude to my brothers and sisters in the Work of Christ Community, for their ongoing love and support. "How good and pleasant it is when brothers live together in unity." (Psalm 133:1).

TABLE OF CONTENTS

| | | | | | | | | | | | | | | | | | | F | ae | ;e |
|--------|------------------------------|----------------------------------|------------|--------------|----------|------------|-------------|----------|----------|---------|---------|--------|---------|---------|----|--------|-----|--------|-----|-----|
| LIST O | F FIG | URES | • | | | | | • | • | • | | • | • | | | • | | • | | v |
| Chapte | r | | | | | | | | | | | | | | | | | | | |
| I. | INTR | RODUCTION | ۷. | | | | | • | | • | | • | | | • | | • | | • | 1 |
| | 1-1 1-2 | Introdi Introdi | uct uct | ion ion | to to | the Ter | r mi | he no | si lo | s gy | • | | • | • | • | | • | | • | 1 2 |
| II. | THE | BOND-GRA | APH | FIN | 1ITE | E-EI | ĿΝ | ΊΕΝ | Т | ME | ТН | OD | • | • | • | | • | • | | 5 |
| | 2 - 1 2 - 2 | The Des Derivat Example | tio | n. | | | | | | • | | | | • | | | • | | | 58 |
| | | 2 - 2.1 2 - 2.2 | | | | | | | | | | | | | | | | | | |
| | 2 - 3 2 - 4 | Applyin Some Si | | | | | | | | | | | | | | | | | | |
| | | 2-4.1 2-4.2 | | gher ree- | | | | | | | | | | | | | | | | |
| III. | | MPARISON INITE-E | | | | | | | | | | | | | | | | S • | . 2 | 9 |
| | | Superpo Boundar Solutio | су | Cond | diti | ions | | | • | • | | • | | | | • | | • | • 3 | 2 |
| IV. | | LUSIONS STIGATIO | | D RE | ECON | MMEN | ID <i>A</i> | TI. | ON • | S : | F0 • | R • | FU • | RT • | HE | R • | | • | • 3 | 9 |
| | 4-1 4-2 | Conclus Recomme | | | | For | | | | er | I | nv | · es | ti | ga | iti | .or | • | .3 | |

| | | | | Pa | age |
|------|---|---|---|----|-----|
| APPI | ENDICES | | | | |
| Α. | Internal Structure Of A Constant-Strain Triangular (6-Port) Element | • | • | | 42 |
| В. | Supporting Mathematics | • | • | | 47 |
| LIST | r of references | • | | | 49 |

LIST OF FIGURES

| Figure | Pa | age |
|----------------|---|------------|
| 1-1. | Constant-strain triangular elastic element with nodal displacements shown | . 4 |
| 1-2. | 6-port C-field representation of elastic element | . 4 |
| 2-1. | Desired form of elastic element model | .22 |
| 2-2. | Model with six external ports, internal 3-port C-field | .22 |
| 2-3. | Model with decoupled C-elements | .22 |
| 2-4. | Axisymmetric rod with exponentially-varying cross-section | .23 |
| 2 - 5. | Bond-graph element model | .23 |
| 2-6. | Bond-graph assembly model | .23 |
| 2-7. | Constant-strain triangular element for example. | .24 |
| 2-8. | Bond-graph model | . 24 |
| 2-9. | | .25 .25 |
| 2-10. | Causality applied to the bond-graph model | . 25 |
| 2-11. | The junction-structure transformation matrix | .26 |
| 2-12. | Linear-strain triangular element | .27 |
| 2-13. | Form of linear-strain triangle bond-graph model | .28 |
| 2-14. | Constant-strain tetrahedral element | .28 |
| 2 - 15. | Form of tetrahedron bond-graph model | .28 |
| 3-1. | Mesh of four triangular elements | . 36 |
| 3-2. | Bond-graph model of element mesh | . 36 |

| Figure | Pa | age |
|--------|---|------|
| 3-3. | Distributed load applied to element mesh | . 37 |
| 3-4. | Discretized nodal forces | . 37 |
| 3-5. | Port causality applied to the global bond-graph model | |
| A-1. | 3-port pseudo-bond-graph model | .46 |
| A-2. | (2 + 1)-port pseudo-bond-graph model | .46 |

CHAPTER ONE: INTRODUCTION

1-1 Introduction to the Thesis

The Finite-Element Method has come into extensive use in the last fifteen years on a wide range of applications from fluid flow and heat transfer to structural analysis. The popularity and utility of this method are due to its facility for converting a complicated problem with various associated nonlinearities and mathematically difficult boundary conditions into a straightforward (albeit large) problem in linear algebra. This approach also adapts the method for easy implementation on the digital computer, which has also enhanced its popularity in industry.

Bond-Graph techniques have emerged in the last ten years as a viable means of modeling dynamic systems. They present a straightforward procedure for deriving system state equations by means of simple modeling rules, which in turn allows one to analyze the dynamic response of the system. They also contain a certain extractable "intuition" for energy flow in a system. Causal rules inherent in bond-graph techniques allow a reasonably straightforward generation of an input/output form for the system model, which is very useful in many applications.

This study employs multiport bond-graph techniques to gain insight into and augment existing finite-element methods. By using a bond-graph modeling approach, an alternative means of analyzing the behavior of a given finite-element mesh will be derived.

For the purpose of this study, we will restrict ourselves to problems in elasticity, with the understanding that the method generated here can be later generalized to other areas of application. We will also restrict our analysis to linear constant-strain, two-dimensional algebra in our bond-graph models, which will allow clearer initial understanding of the new method without sacrificing depth of insight, as well as saving time in unnecessarily involved computations. Again, this is with the understanding that this restriction can be generalized later to include a wider range of problems.

1-2 Introduction to Terminology

In this section, we will introduce some of the notation and terminology which will appear regularly in this thesis. We are concerned in this thesis with developing a bond-graph model of an element used in a finite-element analysis of two-dimensional elasticity.

The typical element used in finite-element analysis is a constant-strain triangular element (Figure 1-1). These elements will fit together in a mesh to approximate the shape and elastic properties of the object being analyzed (e.g. an airplane wing, automobile body, etc.). Typically, in elasticity problems, the primary variables are force and displacement

(deformation) at the element nodes (vertices). These forces and displacements form the nodal force vector, \mathbf{F}_n , and the nodal displacement vector, \mathbf{X}_n , which are related by the global assembly stiffness matrix, as in

$$F_n = K_a X_n$$

In bond-graph terminology, such a stiffness relationship is characteristic of a C-field, which models elastic (or, in a sense, mechanical capacitance) properties of an object (see (1)). We may also speak of the number of 'ports' associated with a given bond-graph element, and this simply refers to the means of energy flow between an element and adjacent elements. A 2-port element, for example, is able to transfer energy along two "paths" (in a bond-graph sense) with adjacent elements. In the case of the constant-strain triangle, it "communicates" with adjacent elements through nodal forces and displacements. In a two-dimensional problem, two linearly independent coordinates are necessary to describe the loading and motion of the node. Each node, then, has two directions (x and y) in which to transfer energy to adjoining elements, and thus, in regard to the elastic properties of the triangular element, we model it as a 6-port C-field (Figure 1-2). Some prior knowledge of bond-graph notation and methodology is assumed. (If such is not the case, please see (1) as a reference).

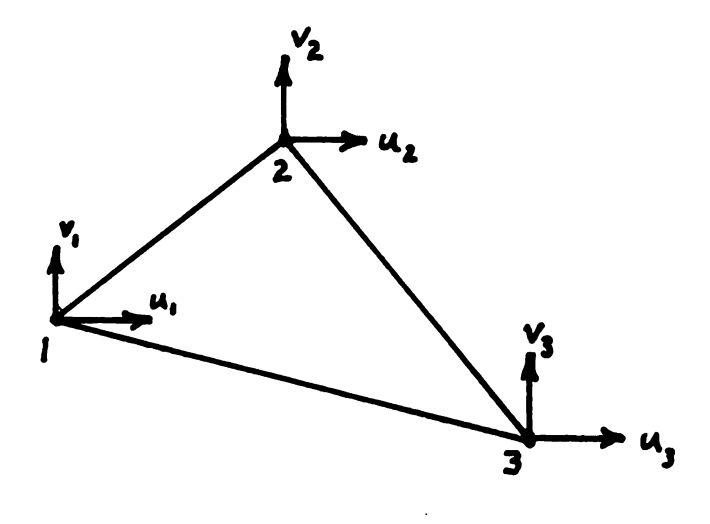


Figure 1-1. Constant-strain triangular elastic element with nodal displacements shown

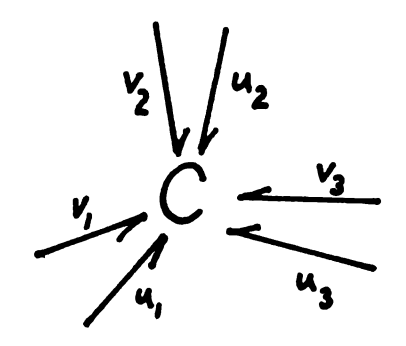


Figure 1-2. 6-port C-field representation of elastic element

CHAPTER TWO: THE BOND-GRAPH FINITE-ELEMENT METHOD

2-1 The Desired Model - Description and Derivation

Our primary motivation here is to develop a means of modeling a finite-element mesh in terms of bond-graph structures so as to take advantage of the strengths of bond-graph techniques. For the elastic elements considered here, we model force as the effort variable and velocity as the flow variable.

In the case of a linear elastic element, then, we would desire a model of the type shown in Figure 2-1, where a junction structure composed of 0- and 1-junctions and TF-elements connects the external ports (inputs, boundary values) to the internal elastic storage field (see (1)). The number of external and internal bonds are determined by the geometry of the problem (i.e., number of element nodes, dimensionality, etc.) and the junction structure is determined by relation—ships between the external and internal ports. This type of model, along with the proper assignment of causality, allows a direct transformation from "input" to "output" for each element, and is the most systematic type of model with which to work.

In Appendix A, we see that the internal structure of a constant-strain triangular element is that of an external 6-port with three internal parts; thus, we will construct

our model along the same pattern of six external and three internal ports (Figure 2-2). Even better would be a model such as the one shown in Figure 2-3, where the 3-port elastic storage field is in the form of three decoupled 1-port C-elements. If such a model is possible, it would allow for a more direct and explicit representation of the element model, as well as being intuitively and analytically easier to work with.

The mathematics of this decoupled model can be derived from the constitutive and connective relationships of the bond-graph structure. Each (linear) C-element has a constitutive equation of the form

$$F_{c} = K_{c}X_{c}$$

relating the force and displacement in the storage element; the constant of proportionality, $K_{\rm c}$, is the stiffness of the C-element. In 3-port form, the 3-port stiffness matrix would be a diagonal matrix whose elements are the individual stiffnesses of each distinct C-, and the constitutive relationship would be

$$\begin{bmatrix}
F_1 & & & K_1 & & 0 & & 0 \\
F_2 & = & 0 & & K_2 & & 0 \\
F_3 & & 0 & & 0 & & K_3
\end{bmatrix}$$

$$\begin{bmatrix}
x_1 \\
x_2 \\
x_3
\end{bmatrix}$$

The junction structure shown in Figure 2-2 would be represented by a 6x3 matrix whose elements would be the moduli of the TF-elements joining the appropriate external and internal

bonds according to the position in the transformation matrix (e.g., the element in the fifth row and second column would indicate the modulus of a transformer connecting the fifth external port to the second internal port). An element whose value is zero would indicate no connection. To model the external 6-port constitutive relationship of the triangular element, the junction structure (J) and stiffness (K) matrices are assembled in the form

$$K_e = JKJ^T$$
, (2-1)

since, when power is directed through the junction structure, the effort (force) transformation is the transpose of the flow (velocity) transformation. Thus, the 6-port element stiffness matrix is expressible as a combination of linear transformations - from external forces through the junction structure to the internal forces; then, by means of the internal constitutive relationships, the internal displacements are transformed into internal displacements, which are mapped through the junction structure into external displacements.

So, we see that we seek a synthesis of the form of (2-1), where K is a diagonal matrix. Such a synthesis can be shown to exist for every K_e (see Appendix B). Any real symmetric matrix A (a condition satisfied by all elastic element stiffness matrices) can be decomposed into a diagonal matrix M, whose elements are the eigenvalues of A and a transformation T, whose columns are the corresponding eigenvectors of A, normalized to unit magnitude, so that

$$A = TMT^{T} . (2-2)$$

We need only consider the non-zero eigenvalues, since any zero eigenvalues will have no effect on the matrix product. In the case of a stiffness matrix K_e for a constant-strain triangular element, M will be 3x3, since K_e will always have at least three zero eigenvalues, due to its construction, (Appendix B) and T, then, will be 6x3.

By correlating equations 2-1 and 2-2 above, we see then that we may construct a bond graph representation of K_e by means of three 1-port C-elements whose stiffnesses are the non-zero eigenvalues of K_e (corresponding to the diagonalized matrix K in equation 2-1) and a junction structure of transformers whose moduli are determined by the corresponding normalized eigenvectors of K_e (corresponding to the matrix J in equation 2-1). This is the core of the modeling method.

2-2 Examples

Some examples will be helpful in demonstrating the method described above.

2-2.1 A One-Dimensional Example

For the sake of computational simplicity, let us begin with a one-dimensional linear 2-port example. This will provide an easy first case, and will allow us easily to demonstrate the junction-structure transformation matrices, as well as to demonstrate how the 1-junction connectors naturally use the principle of superposition for nodal forces. (This example problem is build upon an example given in (2), p. 59).

We consider the case of an axisymmetric rod whose area varies exponentially with length (Figure 2-4). We subdivide the rod into two elements, each of length L, and define

$$A(x) = A_0 e^{-Px}$$
 and $2LP = 1$

so that

$$A_1 = A_0, \quad A_2 = .606A_0, \quad A_3 = .368A_0.$$

Choosing the cross-sectional area for each element as the average of the two nodal areas for that element, we obtain

$$A_{a} = .803A_{1}, A_{b} = .487A_{1}$$

We now find the element stiffness matrices (by standard methods) to be

$$K_a = \begin{bmatrix} .803 & -.803 \\ -.803 & .803 \end{bmatrix} \frac{A_0E}{L} \text{ and } K_b = \begin{bmatrix} .487 & -.487 \\ -.487 & .487 \end{bmatrix} \frac{A_0E}{L}$$

At this point the bond-graph analysis begins.

We first solve for the eigenvalues and eigenvectors of K_a and K_b . K_a has eigenvalues 0 and 1.606. K_b has eigenvalues (not surprisingly) 0 and 0.974. In each case, the normalized eigenvector corresponding to the non-zero eigenvalue is

$$v = \begin{bmatrix} .707 \\ -.707 \end{bmatrix}$$

So, in the case of element a (and similarly for element b) we have

$$K_{a} = \begin{bmatrix} .707 \\ -.707 \end{bmatrix} \begin{bmatrix} 1.606 \end{bmatrix} \begin{bmatrix} .707 & -.707 \end{bmatrix} = \begin{bmatrix} .803 & -.803 \\ -.803 & .803 \end{bmatrix}$$

from which we construct our bond-graph model. By form we can see it will be an external 2-port with one internal port. The stiffness of the internal 1-port C-element will be the eigenvalue (k_a = 1.606), and this internal 1-port capacitance is connected to the two external ports by transformers whose moduli are the elements of the eigenvector, giving us the bond-graph model shown in Figure 2-5.

Now, let us analyze the bond-graph model which we have constructed to show how the model engenders the mathematical construction described above. We have three basic sets of equations; relating the external displacements to internal displacements, we have

$$x_a = .707x_1 - .707x_2$$
;

relating internal forces to external forces,

$$F_1 = .707F_a$$

 $F_2 = -.707F_a$;

and the internal stiffness, relating force to displacement,

$$F_a = 1.606x_a ;$$

which, in a succession of transformations, lead to

$$\begin{bmatrix} F_1 \\ F_2 \end{bmatrix} = \begin{bmatrix} .707 \\ -.707 \end{bmatrix} \begin{bmatrix} 1.606 \\ x_1 \\ x_2 \end{bmatrix}$$

and we see that the product of these transformations is exactly the element stiffness matrix.

Now, having the element models, we wish to assembly them into a global model. At the node, the elements have the same displacement, and forces are additive, which is precisely the definition of a 1-junction in bond-graph modeling. If we connect the separate element models with 1 -junction (thus arriving at the assembly model shown in Figure 2-6), we obtain an assembly stiffness relationship from the 1-junction constitutive law at node 2

$$F_2 = F_{2a} + F_{2b}$$

from which

which is exactly the assembly stiffness matrix generated in finite-element methods by node-wise superposition of element stiffness matrices. We see here, then, that superposition is inherent to the constitutive laws of the 0- and 1-junctions in bond-graph methods.

2-2.2 A Two-Dimensional Example

Here we will consider the case of a single triangular element, as shown in Figure 2-7 (this example was adapted from (3), pp. 109, 115). By standard finite-element methods, (E = $2.9 \cdot 10^7$ psi, μ = 0.3) the stiffness matrix is

$$K_{e} = 1593.4$$

$$9.40 \quad 4.875 \quad -12.5 \quad -5.25 \quad 3.10 \quad 0.375$$

$$4.875 \quad 11.19 \quad -4.50 \quad -4.375 \quad -0.375 \quad -6.81$$

$$-12.5 \quad -4.50 \quad 25.0 \quad 0 \quad -12.5 \quad 4.50$$

$$-5.25 \quad -4.375 \quad 0 \quad 8.75 \quad 5.25 \quad -4.375$$

$$3.10 \quad -9.375 \quad -12.5 \quad 5.25 \quad 9.40 \quad -4.875$$

$$0.375 \quad -6.81 \quad 4.50 \quad -4.375 \quad -4.875 \quad 11.19$$

which would be the stiffness representation for a 6-port model of the element. In order to obtain our more detailed model, we first employ a digital computer to obtain the eigenvalues of K_e , which are 0, 0, 0, 24300, 30960 and 64100, the normalized eigenvectors corresponding to the non-zero eigenvalues are

so we can construct the (3xl)-port-plus-junction-structure model shown in Figure 2-8 (an implied-TF convention has been employed, with the moduli shown in parentheses). With this, our work in terms of the element model is complete. Any further analysis would take place at the assembly level,

connecting a mesh of elements using 1-junctions as shown in section 2-2.1, or applying causality to the model, which is discussed in section 2-3.

It should also be noted that in formulating the model here, we have sacrificed insight into the internal structure of the element (at least in any real, physical sense) for simplicity and directness at a mathematical level. The relationships illustrated in Figure 2-8 don't necessarily have any connection with the internal interactions in any "real" material (see Appendix A). The model shown here was formulated because it is direct, adapts easily to bond-graph methods, and generates the same 6-port stiffness relationship as the standard finite-element technique. As we shall see, however, this may be perfectly adequate.

2-3 Applying Causality to the Model

Causal rules implicit to bond-graph theory can be applied to the method described here to great advantage. Causality greatly facilitates derivation of system state equations and multiport field relationships (see (1) pp. 141-162, 233-258) and will be directly applicable here.

Let us consider the two-dimensional example of section 2-2.2, only let us fix nodes 1 and 3, and apply a 10,000 pound load in the positive x-direction at node 2 (Figure 2-9a) which, in 6-port causal bond-graph form, is as shown in Figure 2-9b. From this causal form, we are able to identify "inputs" to the elastic field as velocities $\dot{\mathbf{u}}_1$, $\dot{\mathbf{v}}_1$, $\dot{\mathbf{u}}_3$, and $\dot{\mathbf{v}}_3$ (all zero) and forces \mathbf{X}_2 (=10K) and \mathbf{Y}_2 (=0), and the "outputs" (to

be solved for) as X_1 , Y_1 , X_3 , Y_3 , U_2 , V_2 . This is a mixed-causal form, as opposed to a strict stiffness form (where all inputs are displacements). We would then desire some direct method for deriving the 6-port field relationship in this mixed-causal "input/output" (I/O) form, i.e.,

Causality allows us to do this directly. If we assign this causality to the expanded model shown in Figure 2-8, as in Figure 2-10, we are able to derive the input/output form from constitutive and connective relationships in the bond-graph, aided by the applied causality.

Immediately we notice that we have a choice in extending the causality inward from the external ports. The derivative causality at \mathbf{y}_2 determines derivative causality at \mathbf{C}_2 , but the derivative causality at \mathbf{x}_2 may be extended to either \mathbf{C}_1 or \mathbf{C}_3 , according to the analyst's choice (in general, a force input would allow a choice between three bonds along which to extend the resulting derivative causality. Also, we see that our model will not allow for more than three force inputs on any given element, as this would result in being unable

to extend the causality inward; physically, it is an underconstrained problem).

If we extend derivative causality to C_1 , C_3 will have integral causality. At this point, we may employ the ENPORT-5 program (4) to obtain a junction-structure matrix, relating inputs and outputs of the junction structure to one another. This matrix is shown in Figure 2-11.

We may then rearrange the information from this matrix into equations of the form

$$F_{op} = A_{11}F_{ip} + A_{12}F_{ic}$$
 $F_{oc} = A_{21}F_{ip} + A_{22}F_{ic}$
 $X_{op} = B_{11}X_{ip} + B_{12}X_{ic}$
 $X_{oc} = B_{21}X_{ip} + B_{22}X_{ic}$

(F and X denote force or displacement vectors; the subscripts 'o' and 'i' denote inputs or outputs to the junction structure; 'c' and 'p' distinguish between the external ports or the internal C-field; i.e. F_{op} is the vector of forces which are outputs at the external ports). The A and B transformation matrices are all taken directly from the JS matrix in Figure 2-11. To these we may add the C-field constitutive relationships

$$F_{ic} = K_i X_{oc}$$

 $X_{ic} = K_d^{-1} F_{oc}$

We may further rearrange these equations into the form

$$F_{op} = A_{11}F_{ip} + A_{12}K_{i}X_{oc}$$
 $X_{op} = B_{11}X_{ip} + B_{12}K_{d}^{-1}F_{oc}$
 $F_{oc} - A_{22}K_{i}X_{oc} = A_{21}F_{ip}$
 $X_{oc} - B_{22}K_{d}^{-1}F_{oc} = B_{21}X_{ip}$

Since, in general, none of the A's or B's are square, we now arrange the last two equations directly above into

$$\begin{bmatrix} I & -A_{22}K_{1} \\ -B_{22}K_{d}^{-1} & I \end{bmatrix} \begin{bmatrix} F_{oc} \\ S_{oc} \end{bmatrix} = \begin{bmatrix} A_{21} & 0 \\ 0 & B_{21} \end{bmatrix} \begin{bmatrix} F_{ip} \\ X_{ip} \end{bmatrix}$$

The large matrix on the left will be square, and, in general, invertible, so we are able to solve for $F_{\rm oc}$ and $X_{\rm oc}$ in terms of $F_{\rm ip}$ and $X_{\rm ip}$, which can in turn be substituted into the first two equations above to complete the solution, ending in the form

$$\begin{bmatrix} F_{op} \\ X_{op} \end{bmatrix} = \begin{bmatrix} X_{ip} \\ F_{ip} \end{bmatrix}$$

(Future development in ENPORT-5 and subsequent versions should condense this procedure).

In our case,

$$K' = \begin{bmatrix} (x_1) & (y_1) & (x_2) & (y_2) & (x_3) & (y_3) \\ .0007 & -3.05 & -.499 & -.601 & .0007 & 3.05 \\ -3.04 & 13030 & -.180 & -.501 & -3.04 & -13030 \\ .499 & .180 & (2.49 \cdot 10^{-5}) & 0 & .499 & -.180 \\ .601 & .501 & 0 & (7.17 \cdot 10^{-5}) & -.601 & .501 \\ .0007 & -3.05 & -.499 & .601 & .0007 & 3.05 \\ 3.04 & -13030 & .180 & -.501 & 3.04 & 13030 \end{bmatrix}$$

(The ports are designated in parentheses above the appropriate column). We may offer a preliminary check on this result by applying the input vector described earlier, with a 10,000 pound force in the x-direction, zero force in the y-direction, and the other four ports fixed, and notice the reaction forces at the fixed vertices. In the x-direction, the reactions are symmetric with respect to the applied force, of opposite direction to the applied force, and very nearly one half as large (we may expect some round-off error). In the y-directions, we note that the forces are symmetric and add to zero also. Further, if a force in the y-direction is applied, the y-reactions add to the negative of the applied force, and the x-reactions add to zero. So, the model is "physically" consistent, and passes the most basic requirement for an acceptable model.

We might also investigate the other possible causal form, with derivative causality extended to C_3 , forcing

integral causality at C_1 . Using the same procedure as demonstrated above, we obtain

$$K'' = \begin{bmatrix} .0007 & -3.05 & -.499 & -.601 & .0007 & 3.05 \\ -3.04 & 13050 & -.180 & -.501 & -3.04 & -13050 \\ .499 & .175 & (2.52 \cdot 10^{-5}) & 0 & .499 & -.175 \\ .601 & .501 & 0 & (7.17 \cdot 10^{-5}) & -.601 & .501 \\ .0007 & -3.05 & -.499 & .601 & .0007 & 3.05 \\ 3.04 & -13050 & .180 & -.501 & 3.04 & 13050 \end{bmatrix}$$

which is, within roundoff error, identical to K'. This is reasonable, since alternative internal causalities do not alter the structure of the model, only (ultimately) the form in which the equations occur. So, it should make no difference how causality is extended within an element, for a given externally-applied causality. This will give some liberty in the actual solution of such problems. (By standard finite-element methods, as described in chapter 3, this matrix would be

8.08.0
$$-.500$$
 $-.599$ 8.08.08.0 13070 $-.180$ $-.499$ -8.0 -13070 .500 $.180$ $(2.5 \cdot 10^{-5})$ 0 $.500$ $-.180$.599 $.499$ 0 $(7.17 \cdot 10^{-5})$ $-.599$ $.499$ 8.0 -8.0 $-.500$ $.599$ 8.0 -8.0 8.0 -13070 $.180$ $-.499$ -8.0 13070

We notice a high degree of correlation here, which would

tend to confirm the accuracy of the bond-graph model.

We see here that we have a relatively straightforward means of deriving a mixed-causal input/output form for our 6-port elastic element, by a natural application of simple causal rules and some linear algebra. This may give the designer a degree of freedom (no pun intended), as will be discussed in chapter three.

A note is worthwhile here concerning finite-element meshes of several elements. The principle described here was presented, for the sake of time and space, for the case of a single 6-port element. The principal of superposition (by means of 1-junction connectors, as in 2-2.1) would provide for the means of joining individual elements into a mesh, and for easy derivation of the global matrix. It would also provide the means of extending externally-applied causality inward. The 1-junctions provide one constraint on how this is done, in that a given 1-junction must have one and only one flow (velocity) input. Another constraint on allowable extensions of causality comes from the element models themselves, which require that no more than three effort (force) inputs exist for a given 6-port element. These two conditions will not, in general, completely determine the causality of the entire mesh, however. The engineer will, in general, have several choices in assigning causality to the global mesh. This would suggest that we should seek an optimal causalityassignment strategy, which is beyond the scope or intent of this thesis, but a worthwhile topic for further investigation.

2-4 Some Simple Extensions

The Finite-Element Method takes on a wide range of forms, even if one never leaves the field of elasticity. It would behoove us to apply our bond-graph technique to as many of these as possible, and in this section, a few simple extensions will be discussed.

2-4.1 Higher-Order Elements

In some instances, the constant-strain triangular element with which we have been dealing is not the best choice for design purposes. In some instances, a linear-strain, or even higher order, element is preferred. (When higher-order elements are employed, a smaller number of elements are required to achieve similar accuracy.) Linear-strain elements have also been referred to as quadratic elements, since the linear strains result in the edges of the element being deformed parabolically (see Figure 2-12). In order for these quadratic displacement functions to be determined, however, three nodes, rather than two, must exist along each edge. The third node is usually chosen as the "mid-point" of the edge. This gives us a total of six nodes for each element, each capable of motion in two directions, so, externally, the linear-strain triangular element is a 12-port. nally, however, the structure is determined by Hooke's Law, which in two dimensions is a 3x3 relationship. We would thus expect the linear-strain element to be an internal 3-port (as in Figure 2-13), which is the case. So for our model, we would begin with the 12x12 stiffness matrix, and solve

for three non-zero eigenvalues and the corresponding eigenvectors, and proceed as before. The extension is similar to constant-strain rectangular elements, which are external 8-ports, but are also internal 3-ports, or to other higher-order elements, such as linear-strain rectangles, etc. In general, for a two dimensional element having n nodes, the element will be an external 2n-port, but will always be an internal 3-port.

2-4.2 Three-Dimensional Elements

The basic three-dimensional element is s constant-strain tetrahedron (see Figure 2-14). Having four nodes each capable of moving in three linearly-independent directions, it is an external 12-port. Its internal response is determined, as always, by Hooke's Law, which, in three dimensions, is a 6x6 relationship. Thus, we would expect an internal 6-port, or, in terms of our model, six non-zero eigenvalues of the stiffness matrix which determine the stiffness of six internal C-elements, and the corresponding eigenvectors which determine the junction structure connecting the external ports to the internal C-field, as in Figure 2-15.

Higher-order elements may also be used in three dimensions such as constant-strain octahedra or cubes, or linear or quadratic-strain elements, etc. In general, a three-dimensional element having n nodes will be an external 3n-port, while remaining an internal 6-port, due to Hooke's Law, and the modeling procedure would be similar to that delineated above.

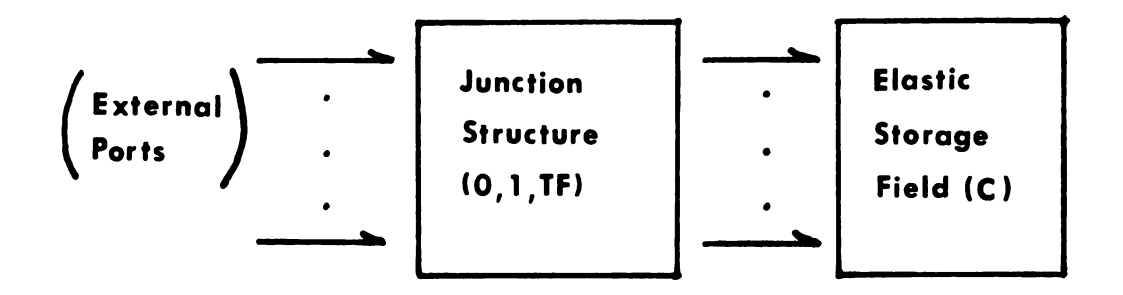


Figure 2-1. Desired form of elastic element model

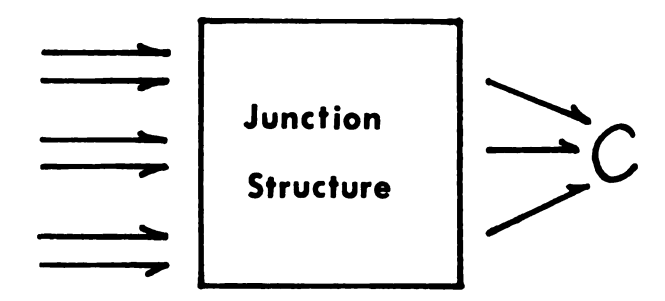


Figure 2-2. Model with six external ports, internal 3-port C-field

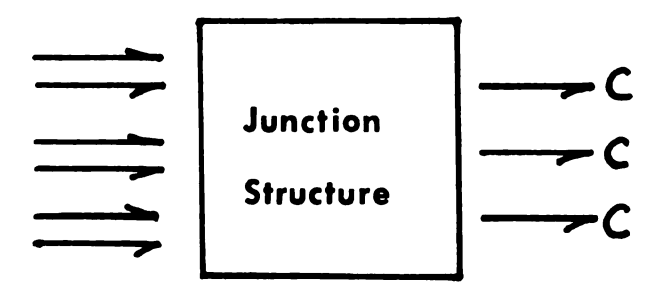


Figure 2-3. Model with decoupled C-elements

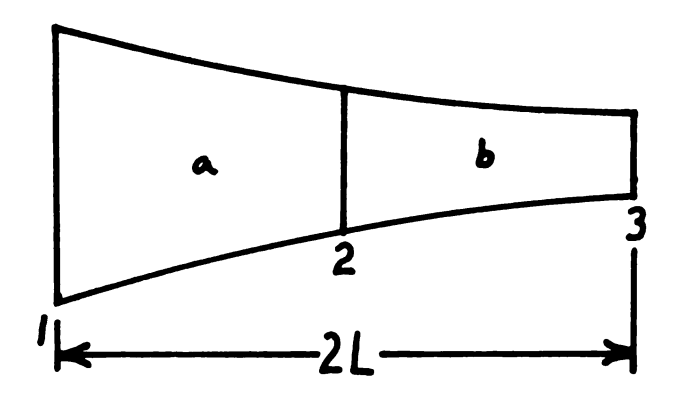


Figure 2-4. Axisymmetric rod with exponentially-varying cross-section

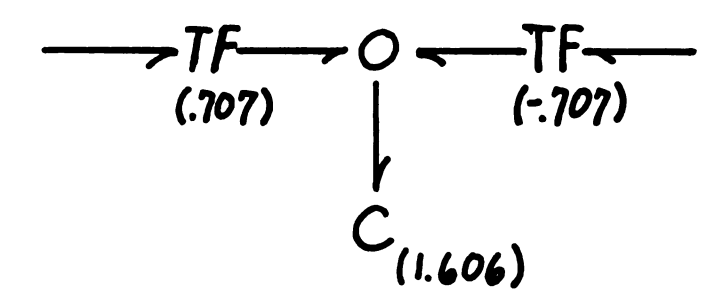


Figure 2-5. Bond-graph element model

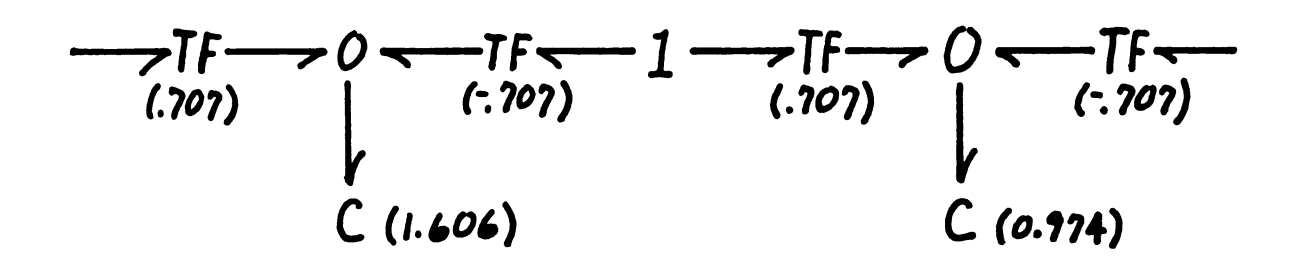


Figure 2-6. Bond-graph assembly model

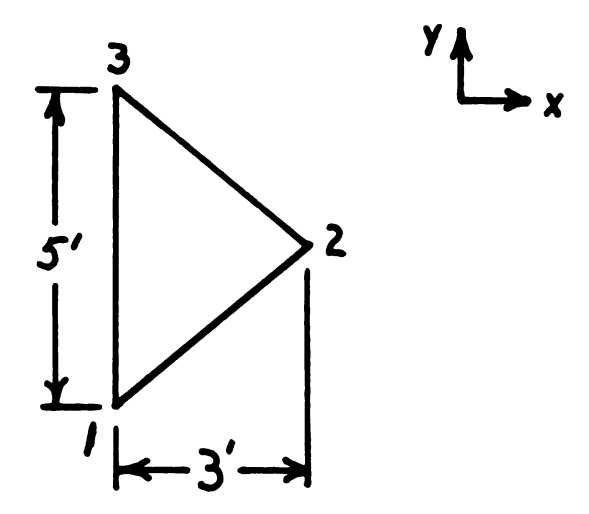


Figure 2-7. Constant-strain triangular element

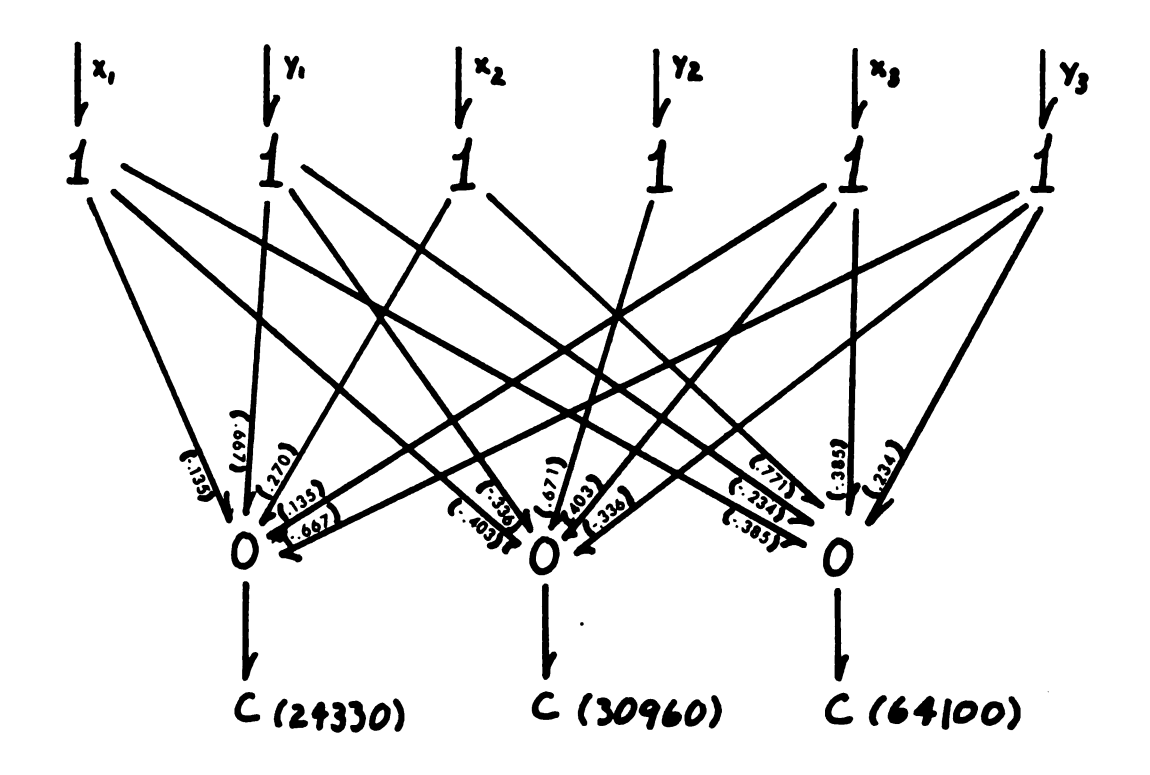


Figure 2-8. Bond-graph model

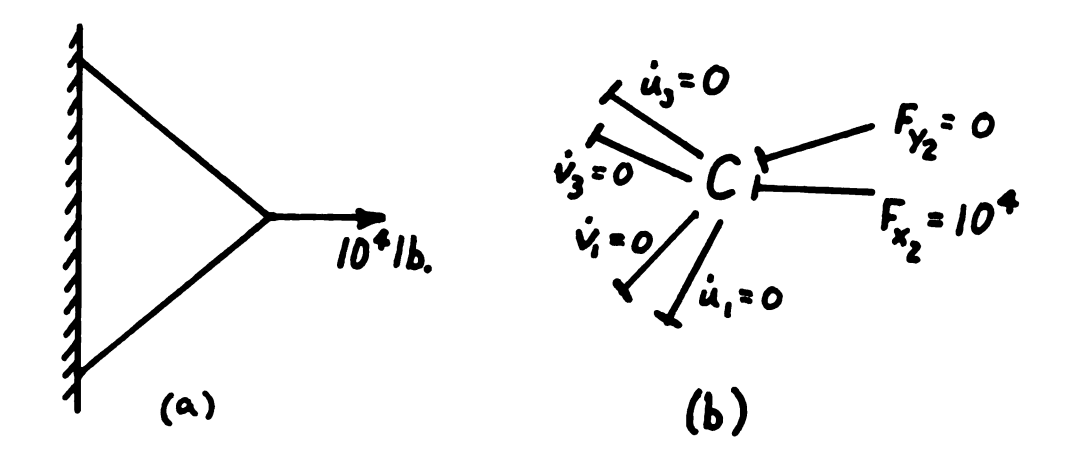


Figure 2-9. (a) Boundary conditions applied to triangular element

(b) 6-port causal bond-graph model

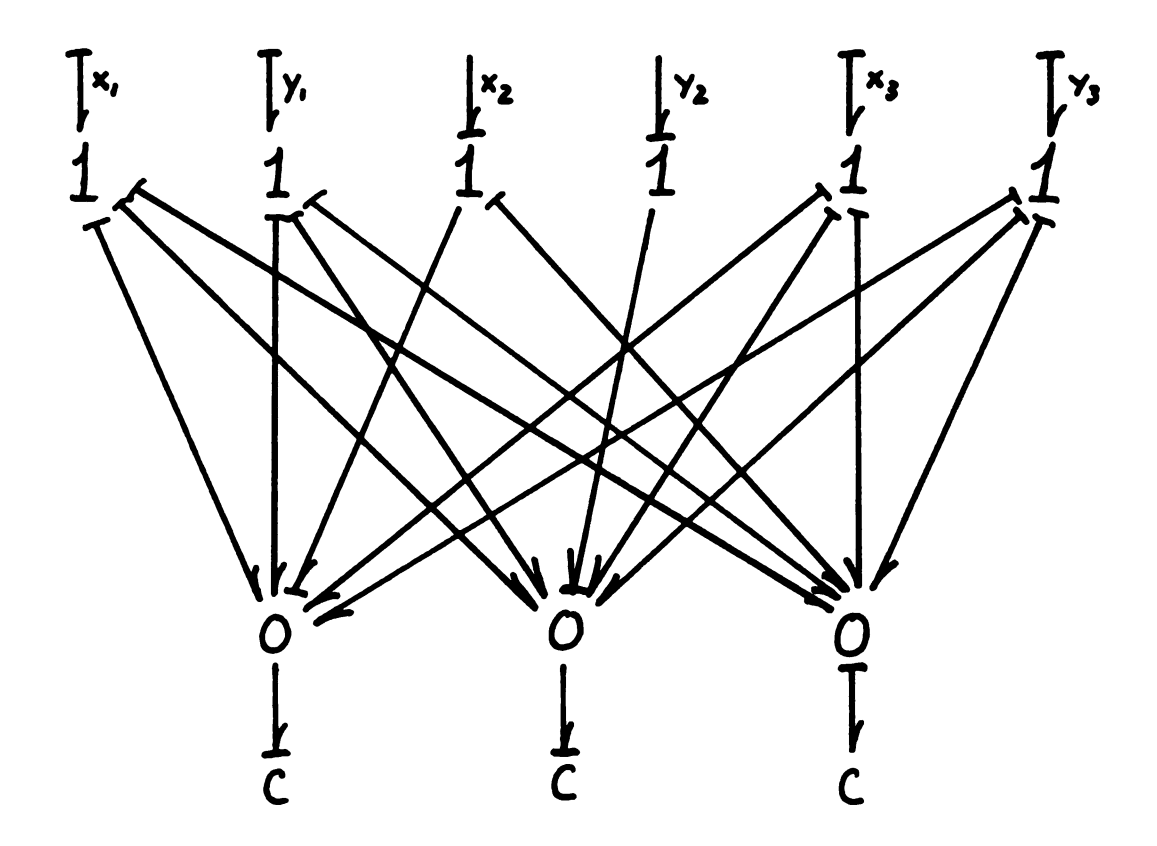


Figure 2-10. Causality applied to the bond-graph model

| | | 0 | 0 | 0 | 0 | 0 | 500 | 601 | .0005 |
|----|-------|-------|-------|------|------|------|-------|------|-------|
| | 0 | 0 | 0 | 0 | 0 | 0 | 2.47 | 501 | -2.14 |
| | 0 | 0 | 0 | 0 | 0 | 0 | 500 | .601 | .0005 |
| | 0 | 0 | 0 | 0 | 0 | 0 | -2.47 | 501 | 2.14 |
| JS | 0 | 0 | 0 | 0 | 0 | 0 | 3.70 | 0 | -2.86 |
| | 0 | 0 | 0 | 0 | 0 | 0 | 0 | 1.49 | 0 |
| | .500 | -2.47 | .500 | 2.47 | 3.70 | 0 | 0 | 0 | 0 |
| | .601 | .501 | 601 | .501 | 0 | 1.49 | 0 | 0 | 0 |
| | .0005 | -2.14 | .0005 | 2.14 | 2.86 | 0 | 0 | 0 | 0 |
| | ا | | | | | | | | 1 |

Figure 2-11. The junction-structure transformation matrix

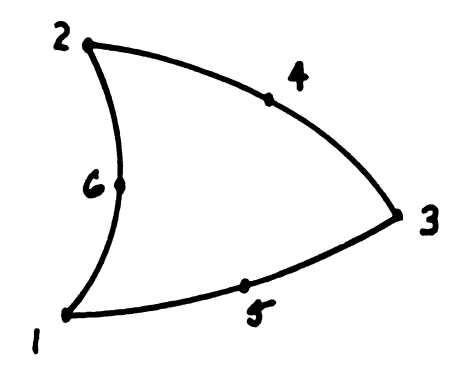


Figure 2-12. Linear-strain triangular element

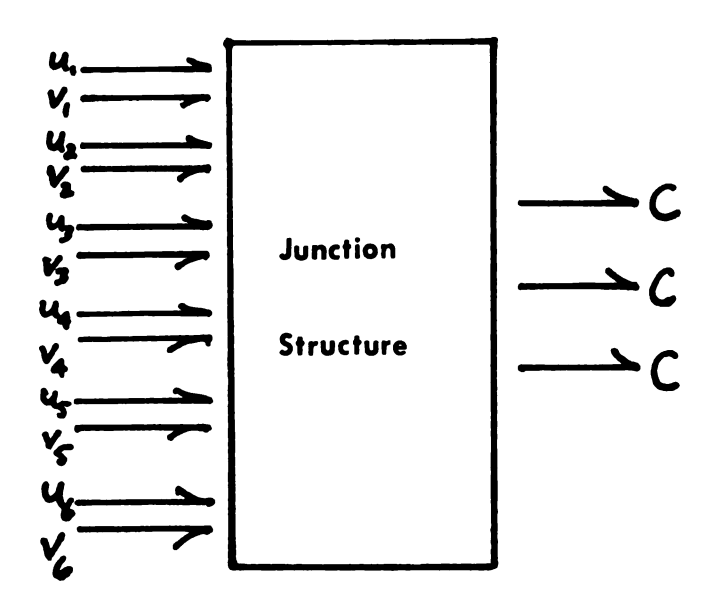


Figure 2-13. Form of linear-strain triangle bond-graph model

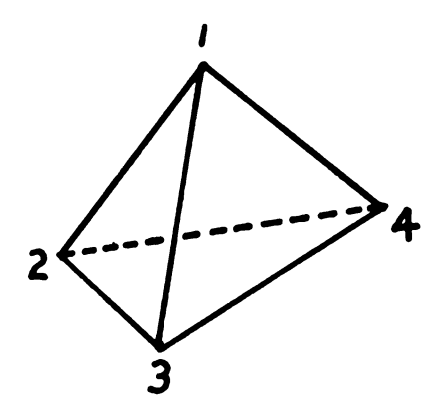


Figure 2-14. Constant-strain tetrahedral element

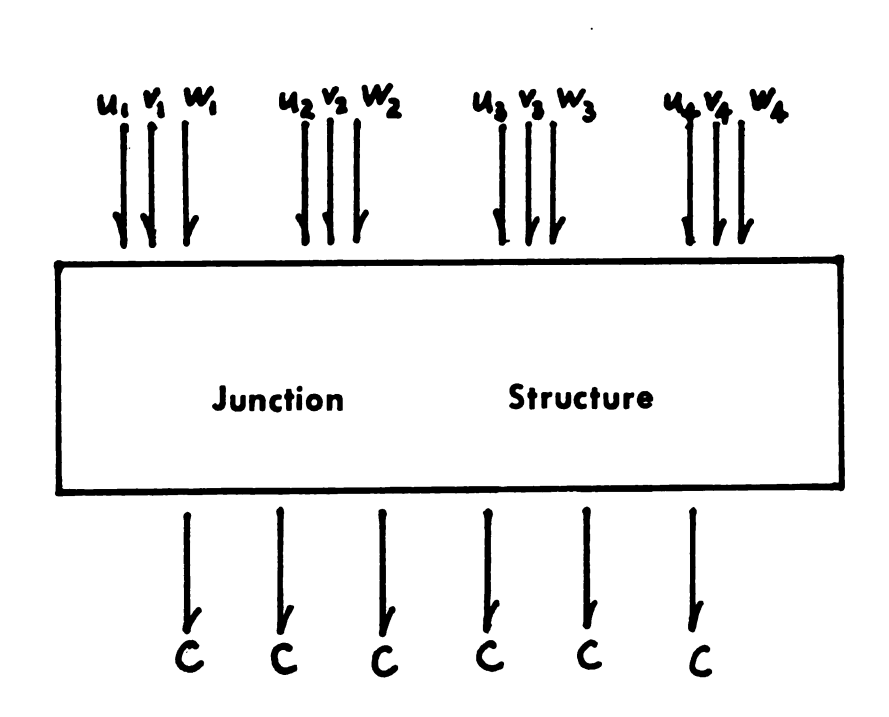


Figure 2-15. Form of tetrahedron bond-graph model

CHAPTER THREE: A COMPARISON OF STANDARD AND BOND-GRAPH METHODS IN FINITE-ELEMENT ANALYSIS

In this chapter we will proceed through the solution process of a typical finite-element problem using both standard finite element methods and the bond-graph method developed in chapter two in a side-by-side fashion, in order to offer a step-by-step comparison. This will demonstrate how various processes "translate" from one method to another, and also how the bond-graph method may be applied to advantage.

For this analysis, we assume prior knowledge of the element mesh for a given problem, and of the individual element stiffness matrices. Knowing the element stiffness matrices, we are able then to formulate bond-graph models for each of the elements, as delineated in section 2-1 and demonstrated in section 2-2.2. From this point, we will proceed through three steps to final solution of the problem: superposition of element stiffness matrices to form the assembly stiffness matrix, application of boundary conditions, and the final steps to the solution of the problem.

3-1 Superposition

Let us consider the element mesh shown in Figure 3-1, with known element stiffness matrices. (This is taken from (3), pp. 109-124). Its bond-graph model is shown in

Figure 3-2, with element models shown in basic 6-port form (to show the full model would result in an extremely cluttered drawing; visualize these basic 6-ports as being detailed models as shown in chapter two). We note that each node in the element mesh is represented by two 1-junctions in the bond-graph model. Once again, this is because each 1-junction represents a common flow (velocity), and each node is free to move in two linearly independent directions. At each node, the elements meeting at that node will have velocity and displacement in common, hence 1-junctions are used to connect the elements in a mesh.

Now, by standard finite-element methods, when the assembly stiffness matrix is desired, a node-wise superposition of element stiffness matrices is performed. The stiffness matrices are subdivided into 2x2 submatrices describing the effect of a displacement at one node on the force at another node, as in

$$K_{1} = \begin{bmatrix} K_{11} & K_{12} & K_{13} \\ K_{21} & K_{22} & K_{23} \\ K_{31} & K_{32} & K_{33} \end{bmatrix}_{1}$$
, $K_{2} = \begin{bmatrix} K_{22} & K_{23} & K_{24} \\ K_{32} & K_{33} & K_{34} \\ K_{42} & K_{43} & K_{44} \end{bmatrix}_{2}$, etc.

These 2x2 matrices are then added according to subscript to produce the global stiffness matrix,

$$K_{g} = \begin{bmatrix} \Sigma K_{11} & \Sigma K_{12} & \Sigma K_{13} & \Sigma K_{14} & \Sigma K_{15} \\ \Sigma K_{21} & \Sigma K_{22} & \Sigma K_{23} & \Sigma K_{24} & \Sigma K_{25} \\ \Sigma K_{31} & \Sigma K_{32} & \Sigma K_{33} & \Sigma K_{34} & \Sigma K_{35} \\ \Sigma K_{41} & \Sigma K_{42} & \Sigma K_{43} & \Sigma K_{44} & \Sigma K_{45} \\ \Sigma K_{51} & \Sigma K_{52} & \Sigma K_{53} & \Sigma K_{54} & \Sigma K_{55} \end{bmatrix}$$

In the bond-graph method, this process is inherent to the 1-junction connectors. As well as connoting common flow (velocity), 1-junctions connote a summation of forces. For example, at node 2

$$\begin{bmatrix} x_{2} \\ y_{2} \end{bmatrix} = \begin{bmatrix} x_{2} \\ y_{2} \end{bmatrix}_{1} + \begin{bmatrix} x_{2} \\ y_{2} \end{bmatrix}_{2}$$

$$= K_{21-1} \begin{bmatrix} u_{1} \\ v_{1} \end{bmatrix} + K_{22-1} \begin{bmatrix} u_{2} \\ v_{2} \end{bmatrix} + K_{23-1} \begin{bmatrix} u_{3} \\ v_{3} \end{bmatrix}$$

$$+ K_{22-2} \begin{bmatrix} u_{2} \\ v_{2} \end{bmatrix} + K_{23-2} \begin{bmatrix} u_{3} \\ v_{3} \end{bmatrix} + K_{24-2} \begin{bmatrix} u_{4} \\ v_{4} \end{bmatrix}$$

$$= K_{21-1} \begin{bmatrix} u_{1} \\ v_{1} \end{bmatrix} + (K_{22-1} + K_{23-2}) \begin{bmatrix} u_{2} \\ v_{2} \end{bmatrix} + K_{24-2} \begin{bmatrix} u_{4} \\ v_{4} \end{bmatrix}$$

$$(K_{23-1} + K_{23-2}) \begin{bmatrix} u_{3} \\ v_{3} \end{bmatrix} + K_{24-2} \begin{bmatrix} u_{4} \\ v_{4} \end{bmatrix}$$

This occurs similarly for each node in the mesh. So we see that the very definition of a 1-junction as a common-velocity, force-summing connector results in the node-wise superposition of element stiffness matrices. This is a nice feature, in that, in a computational sense, it becomes relatively easy to "book-keep" the superposition of element stiffness matrices directly from the bond-graph.

3-2 Boundary Conditions

The next step, following construction of the assembly stiffness matrix, is to establish proper boundary conditions in the problem formulation. What this amounts to in either standard or bond-graph methods is a proper interpretation of the boundary conditions into suitable terms for solution.

In the standard finite-element method, this simply involves translating forces applied to an object into nodal forces applied on the element mesh. In the case of discrete loads applied to the object, the element mesh may be chosen so that the load occurs at a node. In the case of distributed loads (as in Figure 3-3), the loads are integrated between each node and the midpoints of the edges of the adjacent elements on which the load is applied to derive the appropriate "nodal forces" (Figure 3-4). These nodal forces (not all of which are necessarily known) are then arranged into the "nodal force vector", F_n. This vector appears in the assembly stiffness equation

$$F_n = K_g X_n$$

which is the step immediately proceding solution.

In the bond-graph method, the same discretizing process must take place, since the bond-graph is by nature a lumpedparameter rather than a continuous-distribution model, and each node is treated as a 1-junction pair. It is at this point, however, that the bond-graph contains an added flexibility in assigning external port (boundary) conditions. Causality will permit either force or velocity inputs to the bond-graph (in this static model, we may just as easily speak of displacement, rather than velocity, as an input), which are represented in opposite causal forms. Thus, a load applied at a node may be shown as an effort (force) source to the bond-graph, with the accordant causality, while a displacement input (a pinned joint would be an example of this) may be shown as a flow source, with the opposite causality. Causality thus applied at the external ports may then be extended through the entire assembly of elements (this extension need not be unique, as shown in Figure 3-5). The element constitutive relationships may then be re-evaluated in the appropriate mixedcausal forms and constructed by means of the 1-junction connectors into the mixed-causal assembly constitutive matrix, setting the stage for the final solution.

3-3 Solution

Having constructed the assembly stiffness (or constitutive) matrix and applied the proper boundary conditions, it remains only to finally solve the system for the information which we desire concerning forces and displacements in the assembly.

In standard finite-element methods this begins with the global stiffness equation

$$F_n = K_g X_n$$

which is reorganized into the form ((2), p. 37).

$$\begin{bmatrix} F_{a} \\ F_{b} \end{bmatrix} = \begin{bmatrix} K_{aa} & K_{ab} \\ K_{ab}^{T} & K_{bb} \end{bmatrix} \begin{bmatrix} X_{a} \\ X_{b} \end{bmatrix}$$

where X_a is the vector of known nodal displacements and F_a is the corresponding vector of (unknown) nodal forces, and X_b is the vector of unknown nodal displacements, with F_b the (known) force vector paired with it. Now (if the boundary conditions are such that the assembly is incapable of rigid-body motion, assuring invertibility of K_{bb}) we may solve for X_b :

$$X_b = K_{bb}^{-1} (F_b - K_{ab}^T X_a)$$

which, in turn, allows us to solve for F_a

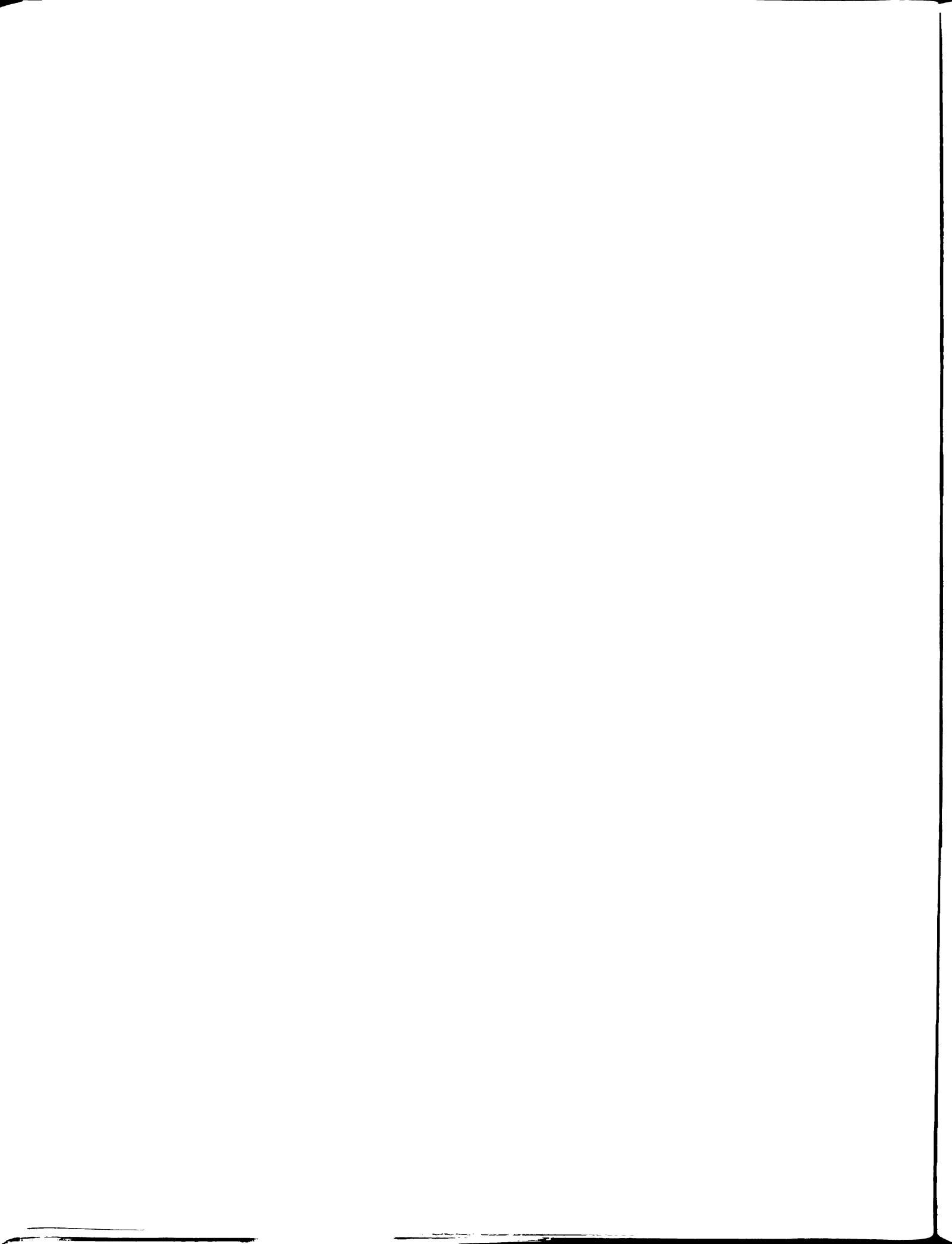
$$F_{a} = (K_{aa} - K_{ab}K_{bb}^{-1}K_{ab}^{T}) X_{a} + K_{ab}K_{bb}^{-1}F_{b}$$

Thus, we have solved for the unknown nodal displacements and the reaction forces at the constraints by essentially an algebraic manipulation of the stiffness equation. By bondgraph methods, we have, in the previous step (by assigning and extending port causality), achieved an assembly constitutive equation of the form (using the previous notation)

$$\begin{bmatrix} F_a \\ X_b \end{bmatrix} = \begin{bmatrix} & & & & \\$$

where we may make a single-pass solution. The matrix K' directly transforms the known (input) vectors \mathbf{X}_a and \mathbf{F}_b into the output vectors \mathbf{F}_a and \mathbf{X}_b , concluding the solution process in one step.

A few comments are worthwhile here concerning this comparison. Standard finite-element methods and bond-graph methods have certain analogous procedures in bringing a problem to solution: 1-junction connectors correspond to superposition of element stiffness matrices, and port causality corresponds to the boundary conditions of the element mesh. The bond-graph technique, though, allows a compression of the solution process. The element models may be constructed and connected to form the assembly model, and causality applied, without any concern for derivation of the assembly constitutive matrix. The assembly matrix may then be derived in mixed-causal form directly from the bond-graph model.



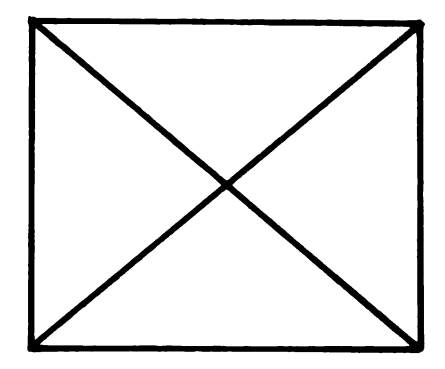


Figure 3-1. Mesh of four triangular elements

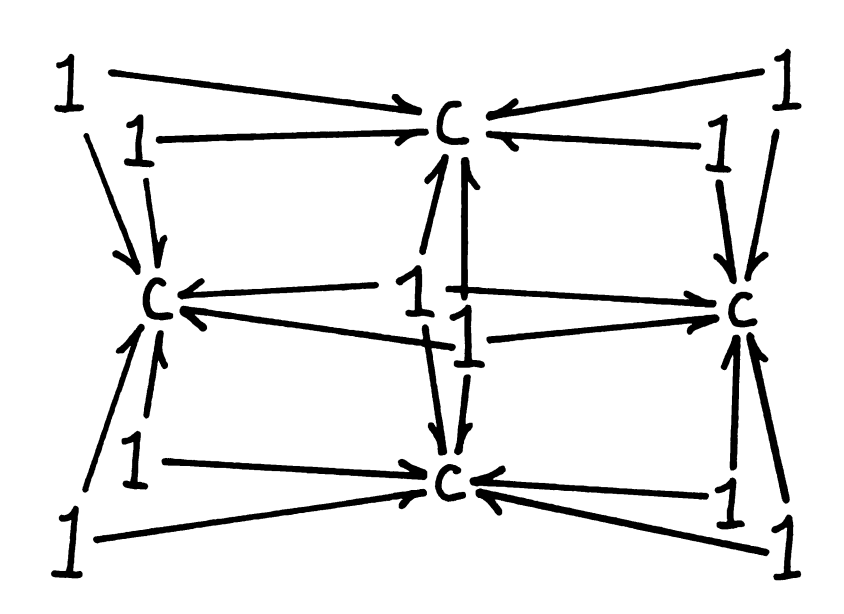


Figure 3-2. Bond-graph model of element mesh

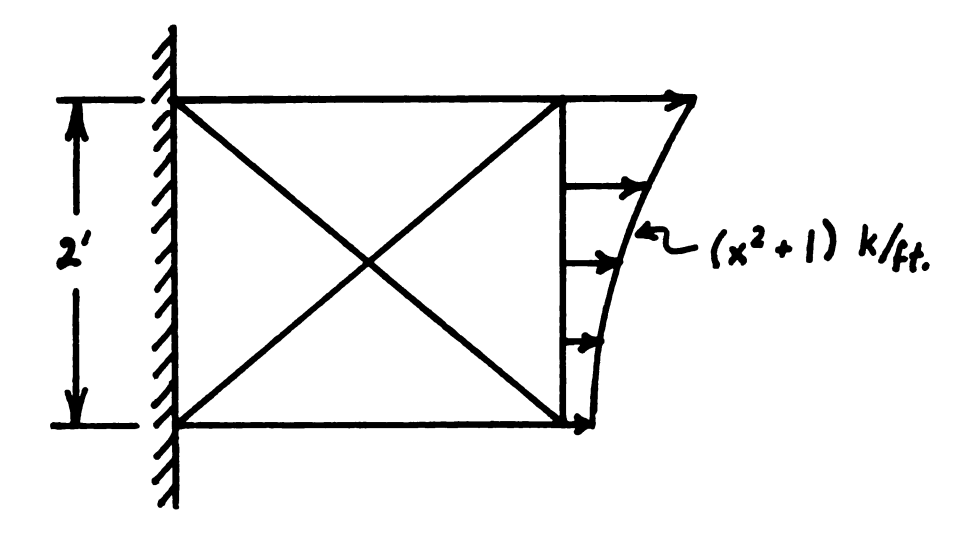


Figure 3-3. Distributed load applied to element mesh

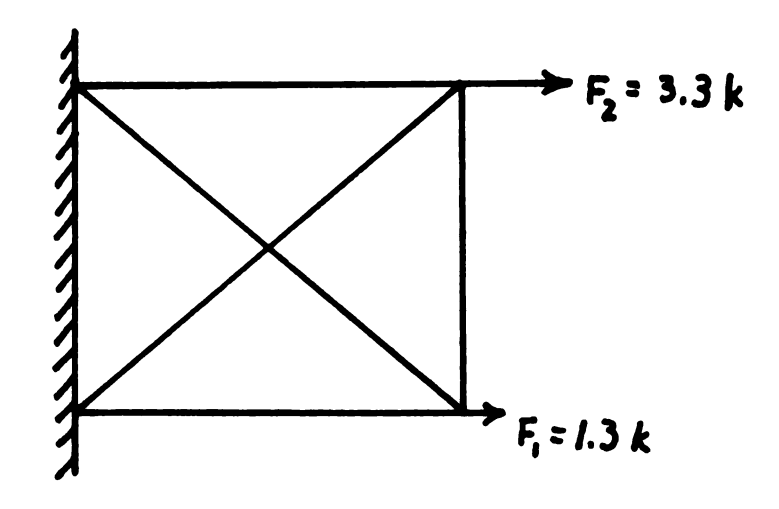


Figure 3-4. Discretized nodal forces

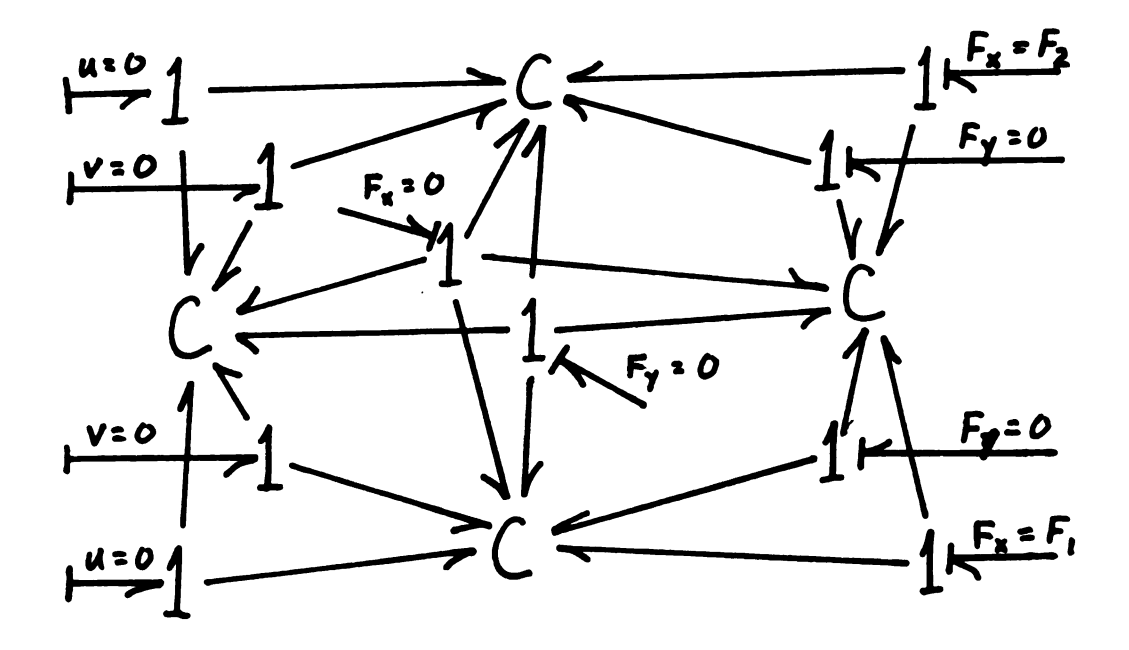


Figure 3-5. Port causality applied to the global bond-graph model

CHAPTER FOUR: CONCLUSIONS AND RECOMMENDATIONS FOR FURTHER INVESTIGATION

4-1 Conclusions

The main result here is to demonstrate that bond-graph techniques can be advantageously applied to problems in finite-element analysis. The model shown here has the property that the 6-port stiffness matrix it generates is identical to that generated by standard finite-element methods, and produces good results for the examples shown. It also has the property that the internal 3-port C-field is represented in the form of three decoupled C-elements, which provides for greater ease in mathematical construction.

Causality applied to the model proved to be a useful tool. It allowed for a direct derivation of element matrices in mixed-causal form, according to the boundary conditions. This made the derivation of the mixed-causal assembly matrix a much more direct problem.

One perhaps hidden advantage of the bond-graph model is that it is "self-contained", so to speak. The elements of the bond-graph are well-defined in mathematical terms, and the generation of the bond-graph model leads fairly directly to the derivation of the relevant equations - in other words, the model "contains" the equations, and the equations are a direct

product of the model. So, a model such as this, the form of which is well known, could be used to advantage.

4-2 Recommendations for Further Investigation

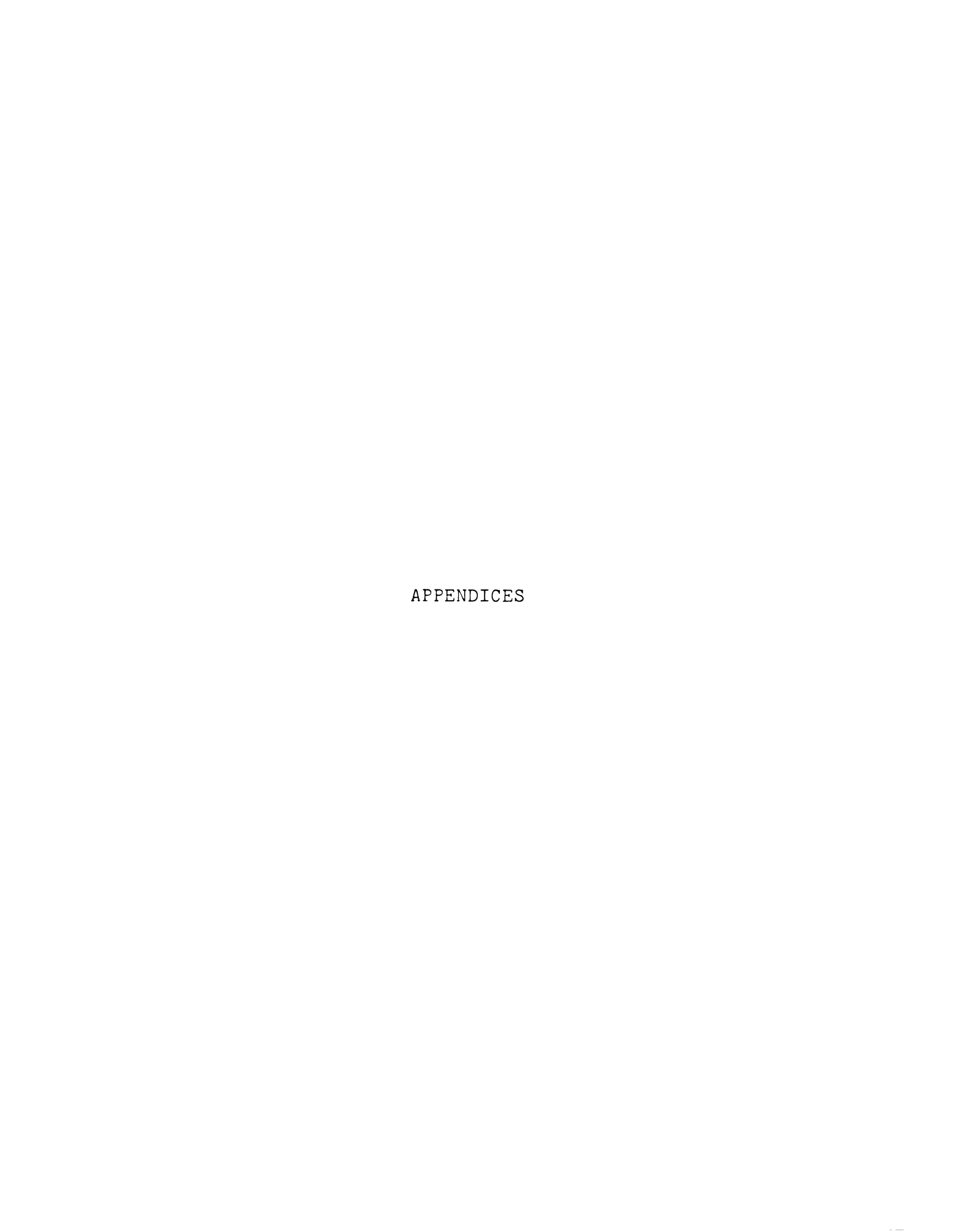
This thesis represents only the first attempt at modeling finite-element methods with bond-graphs; there are many possible directions which could be taken from this point. Certainly effort should be made to improve and streamline the method proposed here, as well as test its accuracy and usefulness in several situations. One particular manner in which this method may be improved would be to achieve a more direct method of deriving the bond-graph model from the finite-element mesh. That is, construct the bond-graph directly from the element mesh, rather than from the element stiffness matrices (which are themselves constructed by standard finite-element techniques), eliminating a step in the modeling process, thereby improving the efficiency of the method. This may involve construction of a different model - the one shown here need not be considered a unique representation.

The model shown here could potentially be used in conjunction with the ENPORT-5 program now being developed. (5) presents the MACRO-element approach to bond-graph modeling incorporated into ENPORT-5. With each 6-port elastic element modeled in this MACRO-element fashion, ENPORT-5 could perform finite-element analysis in a very direct fashion. Further investigation should be made in this direction, as well as how to improve and streamline the procedure.

Bond-graph methods are at their best when modeling dynamic systems, which was not the case here. However, finite-element methods are already being applied to problems in vibration analysis, (see (6), chapter 11) and it is in this direction that the bond-graph techniques hold perhaps their greatest potential. This would involve developing a model for the 6-port I-field necessary for such problems, as well as other steps in assembling a system model and deriving and solving state equations.

A strategy for extending causality into the element mesh might also be considered. For a given mesh of elements, a number of causal forms are possible, and it would be worthwhile to consider which, if any, are preferred.

Finite-element analysis is applied to many different fields of investigation, including heat transfer and fluid flow, as well as various types of elasticity problems, including plate bending and torsion. By proper definition of variables and construction of a suitable model (which may or may not be analogous to the model shown here), bond-graph techniques could be extended to these various problems.





APPENDIX A. INTERNAL STRUCTURE OF A CONSTANT-STRAIN TRIANGULAR (6-PORT) ELEMENT

A constant-strain triangular element could be modeled in bond-graph terms as a general 6-port C-field (Figure 1-2) for a first approximation, since it has three vertices (nodes) each capable of motion in two linearly independent directions (as in Figure 1-1). Each nodal displacement in either the x- or y-direction corresponds to an external port on the 6-port C-field, and the constitutive relationship would take the form

$$F_n = K_e X_n$$

where \mathbf{F}_n is the vector of nodal forces, $\mathbf{K}_e \text{ is the element stiffness matrix}$ and \mathbf{X}_n is the vector of nodal displacements

Given the element stiffness matrix K_e, this could be an adequate model of the element at one level. Since elements are connected to each other by means of common nodal displacements, we could connect the elements to each other in the bond-graph model by means of (common-velocity, force-summing) l-junctions, and thus arrive at a bond-graph model for the element mesh which perfectly describes the finite-element mesh. The l-junction connections implicitly describe the superpositon of element stiffness matrices into the assembly (global) stiffness matrix, which demonstrates some of the power of bond-graph techniques.

This general 6-port model, however, gives no direct information concerning internal structure of the element, or of the effect of alternate causality on the element, or even what causal forms are allowable. For this we need a more detailed model, and we turn to the finite-element construction of the element stiffness matrix to gain our insight.

In standard finite-element techniques, the element stiffness matrix is constructed from

$$K_e = \int_{\mathbf{v}} E^{T} DB dV$$

where B is the strain-displacement matrix which, given nodal displacements, maps them into element strains and D is the matrix mapping strain into stress according to Hooke's Law. A closer look at these matrices will yield insight into the internal structure of the element. We see that B is of the form

which relates strain to displacement according to

$$\varepsilon$$
 = BX

where
$$\varepsilon^{T} = \begin{bmatrix} \varepsilon_{x} & \varepsilon_{y} & Y_{xy} \end{bmatrix}$$
, and $X^{T} = \begin{bmatrix} u_{1} & v_{1} & u_{2} & v_{2} & u_{3} & v_{3} \end{bmatrix}$

so we see that normal strains in the x- and y-directions depend only on displacements in the x- and y-directions, while

shear strains are related to both x and y displacements. Thus, we can model the element in pseudo-bond-graph form as shown in Figure A-1. So we see that we have now reduced our general 6-port model to an internal 3-port C-field model with six external ports. When we consider the constitutive relationship of our 3-port C-field, we recall that

$$\sigma = D \epsilon$$

and from Hooke's Law,

$$D = \frac{E}{1 - \mu^2} \begin{bmatrix} 1 & \mu & 0 \\ \mu & 1 & 0 \\ 0 & 0 & \frac{1 - \mu}{2} \end{bmatrix}$$

$$E = Young's modulus$$

$$\mu = Poisson's ratio$$

Here we see that shear stress is dependent only on shear strain, while normal stresses are related to normal strains in a 2x2 relationship due to Poisson's effect. This allows a further refinement of our 3-port model into a (2 + 1) port model, as in Figure A-2, which is a reasonable model of a constant-strain triangular element, insofar as it allows the extension of externally applied causality into the model,

This model does not have the property that the product of effort and flow variables on each bond is power, since stress and strain are "point" quantities rather than "global" quantities such as force and velocity, and must be volume-integrated to yield proper energy quantities. Such an integration is impossible to represent in bond-graph terms, hence we use a pseudo-bond-graph which endeavors to represent relationships between quantities in bond-graph style to illustrate structure, but is not a true bond-graph.

and gives some degree of information regarding the internal energy structure of the element. This appendix, however, seeks not to specify a model, but to provide information pertinent to the formation of a model, the most important of which is the internal 3-port structure of the 6-port element.

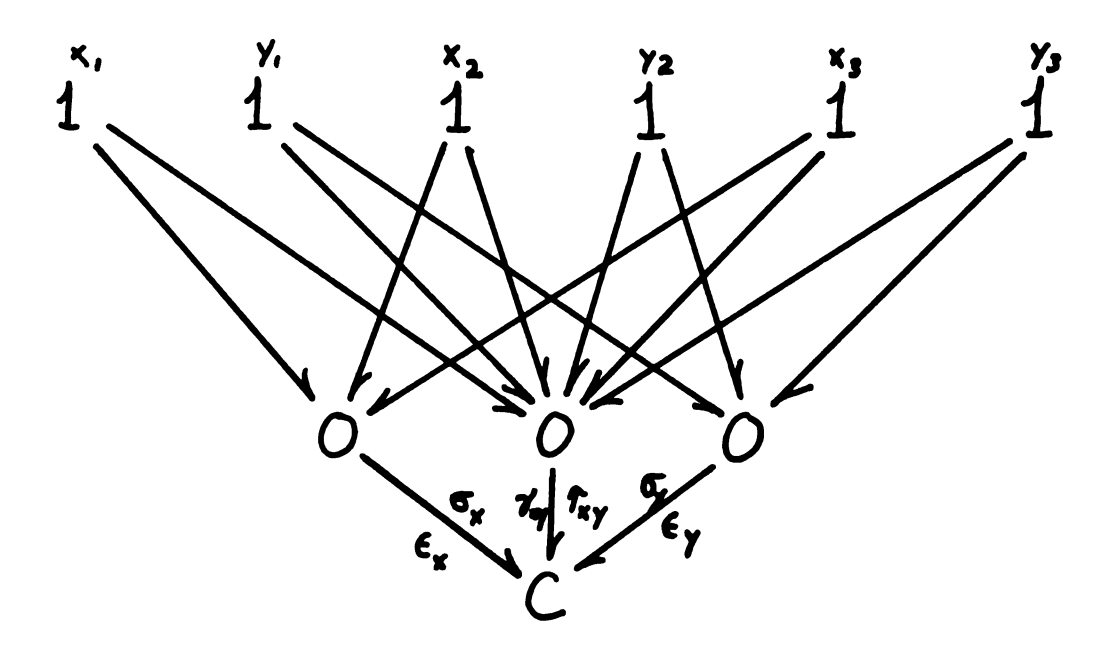


Figure A-1. 3-port pseudo-bond-graph model

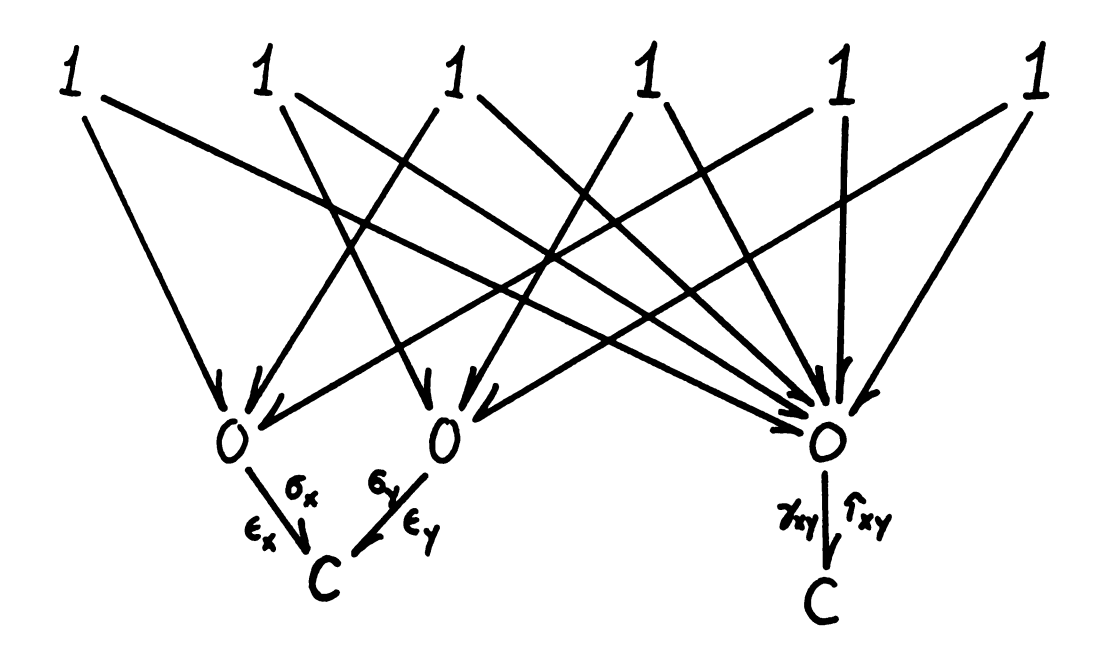


Figure A-2. (2 + 1)-port pseudo-bond-graph model



APPENDIX B. SUPPORTING MATHEMATICS

The key mathematical tool here is a modification of a method for diagonalizing matrices. Any square symmetric real matrix A can be expressed in the form

$$A = M^{-1}LM$$

where L is a diagonal matrix whose elements are the eigenvalues of A, and M is the nodal matrix of A, whose columns are the corresponding normalized eigenvectors of A ((7), pp. 179-183; (8), p. 542). Since this model matrix is orthogonal, we can express

$$M^{-1} = M^{T}$$

so

$$A = M^{T}LM$$

We can further abridge this expression for the case of an element stiffness matrix K_e . It can be shown ((8), pp. 511-512) that since

$$K_e = \int_{\mathbf{v}} B^T DB dV$$

where B and D are both constant matrices having (in the 2 dimensional case) rank 3, that the rank of K_e is 3. (For n-dimensions, K_e will have rank $r = \frac{n(n+1)}{2}$.) From this we can show that K_e has at least three vanishing eigenvalues ((8), p. 549) that K_e can be expressed in the form

$$K_e = M'^T L'M'$$

where L' is the reduced diagonal matrix whose elements are the non-zero eigenvalues of ${\rm K_e}$, and M' is the "semi-modal" matrix whose columns are the eigenvectors corresponding to the eigenvalues in L'.



LIST OF REFERENCES

- 1. Karnopp, D.C. and Rosenberg, R.C. <u>System Dynamics:</u> A Unified Approach. New York: Wiley and Sons, 1975
- 2. Martin, H.C. and Carey, G.F. <u>Introduction to Finite Element Analysis</u>. New York: <u>McGraw-Hill</u>, 1973.
- 3. Ural, O. <u>Finite Element Method</u>. New York: Intext, 1973
- 4. Rosenberg, R.C. Internal Communication, Department of Mechanical Engineering, Michigan State University, 1978
- 5. Devlin, J.E. "Simulation of Engineering Systems Using MACRO Bond-Graph Models", Department of Mechanical Engineering, Michigan State University, M.S. thesis, 1978
- 6. Zienkiewicz, O.C. The Finite Element Method in Structural and Continuum Mechanics. London: McGraw-Hill, 1967.
- 7. Bronson, R. <u>Matrix Methods</u>. New York: Academic Press, 1970
- 8. Wylie, C.R. Advanced Engineering Mathematics. New York: McGraw-Hill, 1975
- 9. Segerlind, L.J. Applied Finite Element Analysis. New York: Wiley and Sons, 1976